14th International Conference on Structural Safety and Reliability - ICOSSAR'25
1-6 June, 2025 - Los Angeles California, USA
R. Ghanem, E. Johnson, S. Masri and A. Olivier (Eds)

CONSIDERATION OF MULTIPLE HAZARDS AND CLIMATE CHANGE IN TIME-DEPENDENT RESILIENCE ASSESSMENT

Cao Wang[1], Bilal M. Ayyub[2], Hao Zhang[3] and Michael Beer[4]

[1] School of Civil and Environmental Engineering,
University of Technology Sydney, Ultimo, NSW 2007, Australia.
Email: cao.wang@uts.edu.au

[2] Center for Technology and Systems Management,
Department of Civil and Environmental Engineering,
University of Maryland, College Park, MD 20742;
International Joint Research Center for Resilient Infrastructure,
Tongji University, Shanghai 200092, China. Email: ba@umd.edu

[3] School of Civil Engineering, The University of Sydney,
Sydney, NSW 2006, Australia. E-mail: hao.zhang@sydney.edu.au

[4] Institute for Risk and Reliability, Leibniz Universität Hannover, Hannover 30167, Germany;
Institute for Risk and Uncertainty, University of Liverpool, Liverpool L69 7ZF, UK;
International Joint Research Center for Resilient Infrastructure &
International Joint Research Center for Engineering Reliability and Stochastic Mechanics,
Tongji University, Shanghai 200092, China. Email: beer@irz.uni-hannover.de

Key words: Time-dependent resilience, multiple hazards, hazard interaction, climate change, performance concern index

Abstract. Civil structures and infrastructure systems are expected to be resilient during their service lives, i.e., they have the ability to be in readiness for, to absorb, recover from and adapt to disruptive events. This is particularly the case when considering the potential impacts of climate change, which may lead to non-stationary natural hazards in the future. Moreover, the presence of concurrent multiple hazards may result in more severe performance reduction to structures/infrastructures, compared with the occurrence of single hazards. In this paper, we will discuss the time-dependent resilience assessment of structures and infrastructure systems exposed to the impacts of concurrent multiple hazards in a changing climate. The interaction between different types of hazards is reflected through the mutual dependency between the performance functions associated with these hazards. We will also address the relationship between the time-dependent resilience and the performance concern index (PCI). Finally, an example is presented to demonstrate the assessment method for time-dependent resilience.

1 INTRODUCTION

Natural hazards are among the major threatening factors for the safety and serviceability of civil structures and infrastructure systems during their service lives [1, 2]. The "resilience" of an object

(e.g., an individual structure, or an infrastructure system consisting of multiple facilities) quantitatively measures the object's ability to withstand, recover from and adapt to the effects of hazardous events. The resilience is typically measured by the integral of performance function within a reference period of interest [3, 4, 5]. A dimensionless measure for resilience, denoted by R_e, was proposed in [6] as follows,

$$R_e = \frac{1}{t_2 - t_1} \int_{t_1}^{t_2} Q(t) dt \tag{1}$$

where $Q(t)$ is the performance function of an object at time t, varying between 0 and 100%, t_1 is the occurrence time of a hazardous event, and t_2 is the time to full recovery (or a user-defined reference time [7]). A generalized resilience measure takes a form of the following [8],

$$R_e = f^{-1}\left[\frac{1}{t_2 - t_1} \int_{t_1}^{t_2} f(Q(t)) dt\right] \tag{2}$$

where $f(x)$ ($x \in [0, 1]$) is a monotonic generating function. If $f(x) \equiv x$, R_e in Eq. (2) reduces to that in Eq. (1). Consider the time-dependent resilience of an object (structure or infrastructure) within a reference period of $[0, t_{sl}]$, denoted by $R_e(0, t_{sl})$ (the term "time-dependent" emphasizes that the resilience is dependent on the time duration under consideration). Extending the model in Eq. (2) with the generating function being $f(x) = \ln x$, the resilience is as follows [8],

$$R_e(0, t_{sl}) = \exp\left[\frac{1}{t_{sl}} \int_0^{t_{sl}} \ln Q(t) dt\right] \tag{3}$$

Note that the performance function $Q(t)$ in Eq. (3) is a stochastic process, with which $R_e(0, t_{sl})$ is a random variable. To achieve a scalar measure, in this paper, we define the resilience as the mean value of $R_e(0, t_{sl})$ in Eq. (3), denoted by $\mathrm{Res}(0, t_{sl})$, that is,

$$\mathrm{Res}(0, t_{sl}) = \mu\left\{\exp\left[\frac{1}{t_{sl}} \int_0^{t_{sl}} \ln Q(t) dt\right]\right\} \tag{4}$$

where $\mu(\,)$ denotes the mean value of the variable in the brackets.

The performance function $Q(t)$ is essentially affected by the hazardous events. Many types of natural hazards display non-stationary characteristics in terms of occurrence frequency and/or magnitude due to the potential impacts of climate change [9]. For example, Ref. [10] projected that the future wind hazard will decrease in Northern Australia, but will increase along the East Coast.

In-service structures and infrastructures are often exposed to the impacts of concurrent multiple hazards [11, 12], instead of single hazard types. The interdependencies of the hazard-induced damaging effects on structures and infrastructures need to be adequately addressed in resilience assessment. Ref. [13] reviewed 17 representative approaches to climate and disaster resilience measurement, and revealed the lack of existing resilience practices that account for the interactions of multiple hazards.

In this paper, we discuss a novel approach for time-dependent resilience assessment of structures and infrastructure systems that are subjected to multiple hazards in a changing climate. The method takes into account the mutual dependency of performance functions associated with different hazard types. We will also discuss the inherent relationship between resilience and the "performance concern index" measuring the asset owner/decision-maker's concern arising from non-full performance (i.e., $Q(t) < 1$). The applicability of the resilience method is illustrated through an example.

2 RESILIENCE MEASURE CONSIDERING MULTIPLE HAZARDS

In the presence of totally m types of hazards (where m is a positive integer), the individual performance associated with the ith hazard type is denoted by $Q_i(t)$ for $i = 1, 2, \ldots m$. The integrated performance considering the combined effects of the m types of hazards, denoted by $Q_{\text{mul}}(t)$, is dependent on the joint behaviour of $Q_1(t), Q_2(t), \ldots Q_m(t)$, and is expressed as follows based on a properly defined function ψ,

$$Q_{\text{mul}}(t) = \psi(Q_1(t), Q_2(t), \ldots Q_m(t)) \tag{5}$$

In Eq. (5), $Q_{\text{mul}}(t)$ takes a value between 0 and 100%, and $Q_{\text{mul}}(t) \leq Q_i(t)$ holds for any i. In this paper, we consider the following formulation of $Q_{\text{mul}}(t)$ (i.e., $\psi = \prod$),

$$Q_{\text{mul}}(t) = \prod_{i=1}^{m} Q_i(t) \tag{6}$$

The determination of each $Q_i(t)$ is dependent on the specific type of hazard and post-hazard damage state of an object, and is generally representative of the asset owner/decision-maker's attitude towards the hazard-induced residual performance.

One numerical example of applying Eq. (6) is presented in Fig. 1, considering two performance functions $Q_1(t)$ and $Q_2(t)$ corresponding to two hazard types. A type-one hazard occurs at time $t = 1$, and a type-two hazard occurs at time $t = 2$. The recovery duration in the aftermath of both events is 2 (i.e., from $t = 1$ to 3 in Fig. 1(a), and from $t = 2$ to 4 in Fig. 1(b)). The integrated performance function, $Q_{\text{mul}}(t)$, is dependent on the joint behaviour of $Q_1(t)$ and $Q_2(t)$, as shown in Fig. 1(c). For example, when $t \in [2, 3]$, $Q_1(t) = Q_2(t) = 0.5$, yielding $Q_{\text{mul}}(t) = Q_1(t) \cdot Q_2(t) = 0.25$.

In Eq. (4), replacing $Q(t)$ with $Q_{\text{mul}}(t)$ in Eq. (6) yields the resilience considering multiple hazards, $\text{Res}_{\text{mul}}(0, t_{\text{sl}})$, as follows,

$$\text{Res}_{\text{mul}}(0, t_{\text{sl}}) = \mu \left\{ \exp \left[\frac{1}{t_{\text{sl}}} \sum_{i=1}^{m} \int_0^{t_{\text{sl}}} \ln Q_i(t) dt \right] \right\} \tag{7}$$

In Eq. (7), if the two performance functions $Q_1(t)$ and $Q_2(t)$ are statistically independent, it follows that,

$$\text{Res}_{\text{mul}}(0, t_{\text{sl}}) = \prod_{i=1}^{m} \text{Res}_i(0, t_{\text{sl}}) \tag{8}$$

in which Res_i is the resilience considering the ith hazard only (evaluated by substituting $Q_i(t)$ into Eq. (4)), $i = 1, 2, \ldots m$. Eq. (8) suggests that, if not considering the mutual dependency between different hazard types, the resilience considering multiple hazards equals the multiplication of the resiliences associated with each hazard type. This observation is consistent with the results in [14]. Illustratively, for the three scenarios in Fig. 1(a–c), based on the three trajectories of performance function, the resiliences for $[0, 6]$ are 0.794, 0.794 and 0.630, respectively (note that $0.794 \times 0.794 = 0.630$), according to Eq. (3).

Note that Eq. (8) does not necessarily hold if considering the mutual dependency between different performance functions. For the case in Fig. 1, at time $t = 2$ when the type-two hazard occurs, if the recovery process is postponed due to the recovery associated with the type-one hazard being in progress, and is resumed at $t = 3$, the "updated" performance function for the type-two hazard, denoted

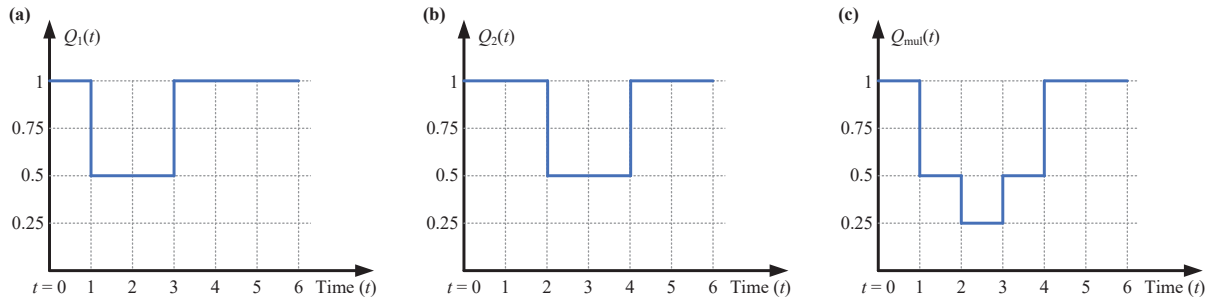

Fig. 1. Time-variation of performance functions. (a) $Q_1(t)$. (b) $Q_2(t)$. (c) $Q_{\text{mul}}(t)$.

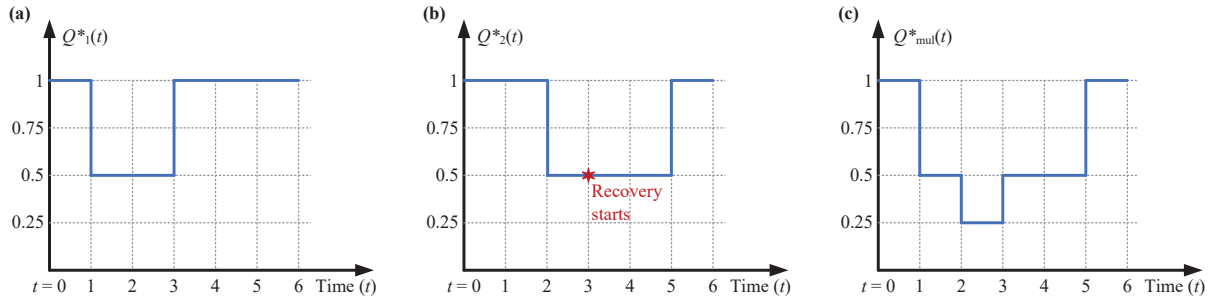

Fig. 2. Time-variation of performance functions considering dependence of $Q_2(t)$ on $Q_1(t)$. (a) $Q_1(t)$. (b) $Q_2^*(t)$. (c) $Q_{\text{mul}}^*(t)$.

by $Q_2^*(t)$, is presented in Fig. 2(b). Correspondingly, the integrated performance function is affected by $Q_2^*(t)$, denoted by $Q_{\text{mul}}^*(t)$ (where the asterisk symbol accounts for the consideration of dependency of $Q_2(t)$ on $Q_1(t)$). The graph of $Q_{\text{mul}}^*(t)$, which equals $Q_1(t) \cdot Q_2^*(t)$, is plotted in Fig. 2(c).

Based on the trajectory in Fig. 2(c), the resilience over $[0, 6]$ is evaluated according to Eq. (3) as 0.561. This is smaller than that associated with Fig. 1(c), implying the impact of performance function dependency on resilience.

Taking into account the mutual dependency between different performance functions, $Q_i(t)$ is modified as $Q_i^*(t)$ for $i = 1, 2, \ldots m$ ($Q_i^*(t) \equiv Q_i(t)$ if the ith performance function is not affected by others; see, e.g., $Q_1(t)$ in Fig. 2(a)), and Eq. (7) is rewritten as follows,

$$\text{Res}_{\text{mul}}(0, t_{\text{sl}}) = \mu \left\{ \exp \left[\frac{1}{t_{\text{sl}}} \sum_{i=1}^{m} \int_0^{t_{\text{sl}}} \ln Q_i^*(t) dt \right] \right\} \tag{9}$$

Eq. (9) presents a method for resilience assessment in the presence of multiple hazards. It has been built on the multiplication-based definition of $Q_{\text{mul}}(t)$ in Eq. (6), and can be extended to fit other definitions in Eq. (5). Note that in Eq. (9), the consideration of climate change impacts on hazardous events can be reflected in the evaluation of each $Q_i^*(t)$, and subsequently in the resilience measure $\text{Res}_{\text{mul}}(0, t_{\text{sl}})$.

3 RELATIONSHIP BETWEEN RESILIENCE AND PERFORMANCE CONCERN INDEX

First, we define the "performance concern index" (PCI), which measures an asset owner/decision maker's concern about the performance of an object (e.g., structure or infrastructure), $Q(t)$. The PCI

at time t, denoted by $\mathbb{C}(t)$, takes a form of

$$\mathbb{C}(t) = -\ln Q(t) = \ln \frac{1}{Q(t)} \tag{10}$$

The PCI in Eq. (10) satisfies the following three conditions simultaneously.

1. A state of full performance (i.e., $Q(t) = 100\%$) leads to no concern.
2. A smaller value of $Q(t)$ means greater concern (i.e., $\mathbb{C}(t)$ is a decreasing function of $Q(t)$).
3. For two independent performance functions, the total amount of concern equals the sum of the concerns associated with the individual performance functions.

One can further show that there is a unique function that satisfies all the three conditions as mentioned above, up to a multiplicative scaling factor.

Denote $\mathbb{C}_{\text{mul}}(t) = -\ln Q_{\text{mul}}(t)$. The average PCI over $[0, t_{\text{sl}}]$, $\overline{\mathbb{C}}_{\text{mul}}$, is evaluated according to

$$\overline{\mathbb{C}}_{\text{mul}} = \frac{1}{t_{\text{sl}}} \int_0^{t_{\text{sl}}} \mathbb{C}_{\text{mul}}(t) dt \tag{11}$$

Based on Eqs. (9) and (11), it follows that,

$$\text{Res}_{\text{mul}}(0, t_{\text{sl}}) = \mu \left[\exp\left(-\overline{\mathbb{C}}_{\text{mul}} \right) \right] \tag{12}$$

Motivated by Eq. (12), we can interpret the resilience problem from an asset owner/decision-maker's concern about the performance function of an object (structure or infrastructure) over its life cycle. Let $\text{nRes}_{\text{mul}}(0, t_{\text{sl}})$ be the time-dependent nonresilience for a reference period of $[0, t_{\text{sl}}]$, which equals $1 - \text{Res}_{\text{mul}}(0, t_{\text{sl}})$. An equivalent form of Eq. (12) is as follows,

$$\text{nRes}_{\text{mul}}(0, t_{\text{sl}}) = \mu \left[1 - \exp\left(-\overline{\mathbb{C}}_{\text{mul}} \right) \right] = 1 - \mu \left[\exp\left(-\overline{\mathbb{C}}_{\text{mul}} \right) \right] \tag{13}$$

In Eq. (13), if $\overline{\mathbb{C}}_{\text{mul}} \approx 0$ (e.g., a well-designed and maintained structure/infrastructure system that raises little concern), we have,

$$\text{nRes}_{\text{mul}}(0, t_{\text{sl}}) \approx \mu(\overline{\mathbb{C}}_{\text{mul}}) \tag{14}$$

which implies that the nonresilience can be approximated by the mean value of the average PCI over a service period of interest.

4 EXAMPLE

In this section, a numerical example, as adopted from [15] with modification, is used to demonstrate the applicability of the resilience model in Eq. (9), and to quantify the impact of performance function dependency on resilience.

Consider a structure subjected to two types of natural hazards, denoted by H1 and H2. The associated performance functions are $Q_1(t)$ and $Q_2(t)$, respectively. For simplicity, assume that the statistics of the hazards and their damaging effects on the structure are identical. For each hazard type, the occurrence is modeled by a non-stationary Poisson process with an occurrence rate of $\lambda(t) = c_0 + c_\lambda t$ (in year^{-1}), in which c_0 is the occurrence rate at the initial time, and c_λ is a constant representing the changing rate of $\lambda(t)$ (note that $c_\lambda = 0$ results in a stationary occurrence process of the hazards).

Conditional on the occurrence of a hazardous event (either type) at time t, the remaining functionality (performance) becomes Q_r times the state immediately before the hazard occurrence. Assume that Q_r follows a Beta distribution with a mean value of $\mu_Q(t)$ (a function of time) and a coefficient of variation (COV) of 0.2. The recovery of functionality immediately after the occurrence of a hazardous event is linear. The recovery rate, K, is dependent on Q_r (i.e., the severity of performance reduction) and resourcefulness, and is expressed as $K = \xi \cdot (0.2 + 2Q_r)$ (in year^{-1}), in which ξ is a constant that reflects the resourcefulness for the recovery process. A reference period of 50 years is considered in this example.

In order to reflect the dependency between the two performance functions, $Q_1(t)$ and $Q_2(t)$, the following three types of dependency are considered.

- Type 0, $Q_1(t)$ and $Q_2(t)$ are mutually independent.
- Type 1, $Q_2(t)$ is affected by $Q_1(t)$ only. Immediately after the occurrence of an H2 event causing reduced $Q_2(t)$, the remaining functionality is further reduced by a factor of η_q, and the recovery process for $Q_2(t)$ is postponed if another recovery associated with H1 is in progress.
- Type 2, $Q_1(t)$ and $Q_2(t)$ affect each other. Immediately after the occurrence of an Hi event causing reduced $Q_i(t)$ ($i = 1, 2$), the remaining functionality is further reduced by a factor of η_q, and the recovery process for $Q_i(t)$ is postponed if another recovery associated with $Q_j(t)$ ($j = 3 - i$) is in progress.

Fig. 3 shows the time-dependent nonresilience (evaluated according to Eq. (9)) for reference periods up to 50 years, considering Types 0, 1 and 2 interaction of $Q_1(t)$ and $Q_2(t)$. The occurrence rate for both hazard types is modeled as $\lambda(t) = 0.1(1 + 0.01t)$, with which the occurrence rate increases by 50% over 50 years. Further, $\eta_q = 0.7$ and $\xi = 1$ (i.e., it needs 5 months to fully restore a 50% functionality). The mean value of Q_r decreases linearly from 0.8 at the initial time to 0.3 by the end of 50 years, with which $\mu_Q(t) = 0.8 - 0.01t$, where t is in years. It is observed from Fig. 3 that, ignoring the performance function dependency will overestimate the resilience of an object, thus yielding a nonconservative evaluation. The nonresilience associated with Type 1 is smaller than that of Type 2, because Type 1 has partially considered the interaction between $Q_1(t)$ and $Q_2(t)$.

Recall that according to Eq. (14), if the nonresilience is close to zero, it can be approximated by the mean value of average PCI. This can be verified by examining the case in Fig. 3. For a reference period of 50 years, the mean value of PCI equals 0.048 and 0.050 for Type 1 and 2, respectively (not shown in the figure), with a difference of only 2.86% and 3.04% compared with the corresponding nonresilience.

In order to investigate the impact of hazard non-stationarity in a changing climate on resilience, the dependence of nonresilience on $\lambda(t)$ and $\mu_Q(t)$ (reflecting the time-variation of hazard magnitude conditional on occurrence) for reference periods up to 50 years is presented in Fig. 4, considering the Type 2 interaction of $Q_1(t)$ and $Q_2(t)$. The configuration is the same as that in Fig. 3 unless otherwise stated. In Fig. 4(a), $c_0 = 0.1$, and the variation of c_λ represents different changing scenarios of the hazard occurrence rate. A greater value of c_λ results in larger nonresilience due to the greater accumulative risks for the structure, and this effect is amplified with a longer reference period. Fig. 4(b) examines four changing patterns for the time-variant mean value of Q_r, that is, $\mu_Q(t)$ decreases linearly from 0.8 at the initial time to 0.5, 0.4, 0.3 and 0.2, respectively over 50 years. A more severe deterioration of the mean value of Q_r, which is representative of amplified hazard intensity over time due to climate change, leads to greater nonresilience. For example, for a reference period of 50 years,

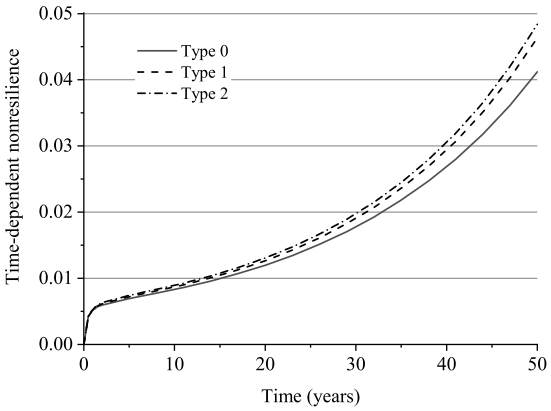

Fig. 3. Time-dependent nonresilience associated with Types 0, 1 and 2 interaction.

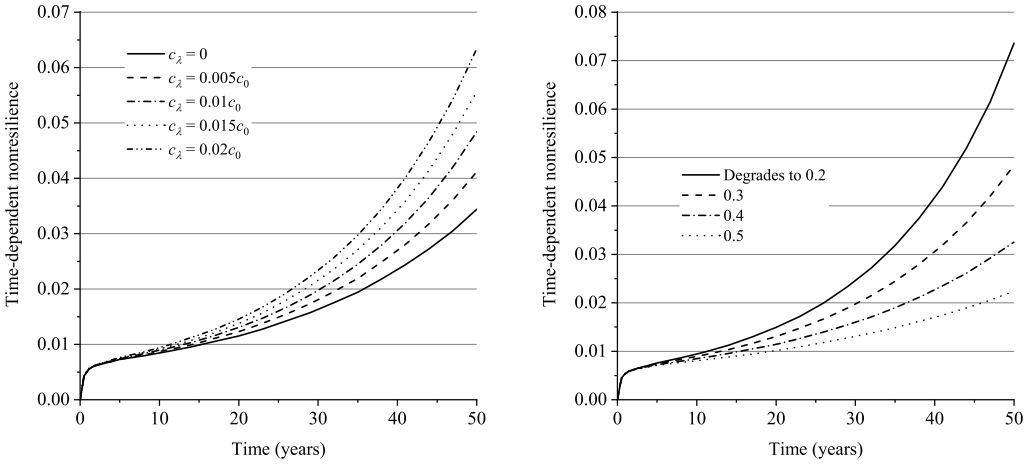

(a) Impact of occurrence rate

(b) Impact of mean value of Q_r

Fig. 4. Impact of hazard non-stationarity on time-dependent nonresilience.

the nonresilience equals 0.022, 0.033, 0.048, and 0.074, respectively, corresponding to the four deterioration scenarios of $\mu_Q(t)$. The observations from Fig. 4 suggest the importance of incorporating the hazard non-stationarity in resilience assessment.

5 CONCLUDING REMARKS

In this paper, we have discussed the evaluation of time-dependent resilience, taking into account the interaction between the performances in response to different types of hazards. The discussed resilience model is applicable to both discrete and continuous hazard processes, and can incorporate the hazard non-stationarity in terms of the hazard intensity and/or occurrence rate due to the potential impacts of climate change.

The performance concern index (PCI), taking a similar form of the Shannon information content, measures an asset owner/decision maker's concern about the performance of an object (structure or infrastructure). The nonresilience, if small enough, can be approximated by the mean value of the average PCI over a considered reference period.

The interaction between the performance functions associated with different types of hazards plays an essential role in resilience assessment. Ignoring such interaction underestimates the nonresilience, thus yielding a nonconservative estimate of an object's performance. Further, resilience assessment needs to incorporate the time-variant characteristics of the hazard intensity and/or occurrence rate in a changing climate.

ACKNOWLEDGEMENTS

C.W. was supported by the Australian Research Council's Discovery Early Career Researcher Award (DE240100207). B.M.A. was supported by the Federal Railroad Administration and the National Oceanic and Atmospheric Administration. These supports are gratefully acknowledged.

REFERENCES

[1] M. C. Gerstenberger, W. Marzocchi, T. Allen, M. Pagani, J. Adams, L. Danciu, E. H. Field, H. Fujiwara, N. Luco, K.-F. Ma, C. Meletti, and M. D. Petersen, "Probabilistic seismic hazard analysis at regional and national scales: State of the art and future challenges," *Rev. Geophys.*, vol. 58, no. 2, p. e2019RG000653, 2020.

[2] C. Wang, H. Zhang, B. R. Ellingwood, Y. Guo, H. Mahmoud, and Q. Li, "Assessing post-hazard damage costs to a community's residential buildings exposed to tropical cyclones," *Struct. Infrastruct. Eng.*, vol. 17, no. 4, pp. 443–453, 2020.

[3] M. Bruneau and A. Reinhorn, "Exploring the concept of seismic resilience for acute care facilities," *Earthquake Spectra*, vol. 23, no. 1, pp. 41–62, 2007.

[4] B. M. Ayyub, "Practical resilience metrics for planning, design, and decision making," *ASCE-ASME J. Risk Uncertainty Eng. Syst., Part A: Civ. Eng.*, vol. 1, no. 3, p. 04015008, 2015.

[5] J. Salomon, M. Broggi, S. Kruse, S. Weber, and M. Beer, "Resilience decision-making for complex systems," *ASCE-ASME J. Risk Uncertainty Eng. Syst., Part B: Mech. Eng.*, vol. 6, no. 2, p. 020901, 2020.

[6] N. O. Attoh-Okine, A. T. Cooper, and S. A. Mensah, "Formulation of resilience index of urban infrastructure using belief functions," *IEEE Syst. J.*, vol. 3, no. 2, pp. 147–153, 2009.

[7] G. P. Cimellaro, A. M. Reinhorn, and M. Bruneau, "Framework for analytical quantification of disaster resilience," *Eng. Struct.*, vol. 32, no. 11, pp. 3639–3649, 2010.

[8] C. Wang, "A generalized index for functionality-sensitive resilience quantification," *Resilient Cities Struct.*, vol. 2, no. 1, pp. 68–75, 2023.

[9] IPCC, *Climate change 2021: The physical science basis*. Contribution of Working Group I to the Sixth Assessment Report of the Intergovernmental Panel on Climate Change. Cambridge University Press, 2021.

[10] K. Walsh, C. J. White, K. McInnes, J. Holmes, S. Schuster, H. Richter, J. P. Evans, A. Di Luca, and R. A. Warren, "Natural hazards in Australia: storms, wind and hail," *Clim. Change*, vol. 139, pp. 55–67, 2016.

[11] Y.-J. Yin and Y. Li, "Probabilistic loss assessment of light-frame wood construction subjected to combined seismic and snow loads," *Eng. Struct.*, vol. 33, no. 2, pp. 380–390, 2011.

[12] M. Bruneau, M. Barbato, J. E. Padgett, A. E. Zaghi, J. Mitrani-Reiser, and Y. Li, "State of the art of multihazard design," *J. Struct. Eng.*, vol. 143, no. 10, p. 03117002, 2017.

[13] F. Laurien, J. G. Martin, and S. Mehryar, "Climate and disaster resilience measurement: Persistent gaps in multiple hazards, methods, and practicability," *Clim. Risk Manage.*, p. 100443, 2022.

[14] C. Wang, B. M. Ayyub, and A. Ahmed, "Time-dependent reliability and resilience of aging structures exposed to multiple hazards in a changing environment," *Resilient Cities Struct.*, vol. 1, no. 3, pp. 40–51, 2022.

[15] C. Wang, "Role of recovery profile dependency in time-dependent resilience," *Eng. Rep.*, p. e12716, 2023.